An Approach for Alignment, Mounting and Integration of IXO Mirror Segments

Kai-Wing Chan*[a,b], William Zhang[b], Timo Saha[c], David Robinson[d], Lawrence Olsen[b], Ryan McClelland[d,e], James Mazzarella[b,e], Lawrence Lozipone[b,e], John Lehan[a,b], Melinda Hong[b,e], Charles Fleetwood[c,e], Tyler Evans[b,e], Glenn Byron[d,e], Jacob Larimore[f]

[a]Center for Research and Exploration in Space Science and Technology & Center for Space Science and Technology, University of Maryland, Baltimore County, Baltimore MD 21250, USA
[b]X-Ray Astrophysics Laboratory, NASA/Goddard Space Flight Center, Greenbelt, MD 20771, USA
[c]Optics Branch, NASA/Goddard Space Flight Center, Greenbelt, MD 20771, USA
[d]Mechanical Engineering Branch, NASA/Goddard Space Flight Center, Greenbelt, MD 20771, USA
[e]SGT, Inc., 7701 Greenbelt Road, Greenbelt, MD 20770, USA
[f]Missouri University of Science and Technology, Rolla, MO 65409

ABSTRACT

The telescope on the International X-ray Observatory (IXO) comprises nearly 15 thousand thin glass mirror segments, each of them is capable of reflecting board-band soft x-rays at grazing angles. These mirror segments form densely packed, two-staged shells, in a Wolter type I optical design, in which each pair of the mirrors focus x-ray onto the focal plane in two reflections. The requirement in angular resolution of the IXO telescope is 5 arc-seconds. This requirement places severe challenges in forming precisely shaped mirror segments as well as in aligning and mounting these thin mirrors, which are 200 to 400 mm in size and 0.4 mm in thickness. In this paper, we will describe an approach for aligning and mounting the IXO mirror segments, in which no active adjustment is made to correct for any existing figure errors. The approach comprises processes such as suspension of a mirror under gravity to minimize gravity distortion, temporary bonding onto a strongback, alignment and transfer to a permanent structure and release of mirror from the temporary mount. Experimental results and analysis in this development are reported.

Keywords: X-ray optics, International X-ray Observatory, IXO telescope, mirror mounting

1. INTRODUCTION

The proposed mission International X-ray Observatory (IXO) aims to make significant discoveries in astrophysics with high-resolution imagining spectroscopy[1], by combining a high-resolution detector and a large telescope with significantly more effective area in the soft x-ray band, from 0.6 – 10 keV, than any of the previous x-ray missions such as Chandra or XMM-Newton has. (For general mission concepts, see also references [2-4]). To provide the large effective area of the soft x-ray telescope, segmented, grazing incidence, Wolter type I optics, is the optics of choice for the mission.

The challenge in the IXO optics lies in meeting the requirement in angular resolution, while satisfying the requirement in having a large effective collecting area and in meeting the mass limit of the launch vehicle. The basic approach is to build a segmented telescope that is assembled from individual modules consisting of densely packed mirror shells. The mirror modules, in turn, are built from aligning and integrating mirror segments in separate processes. Currently, at NASA's Goddard Space Flight Center, the telescope's baseline design, a telescope with a diameter of 3.2 m (outermost x-ray reflecting shell) and consisting of about 15 thousand thin 0.4 mm glass mirror segments, does satisfy the area requirement within the mass budget. Nevertheless, within these limits, the mirror surface area and mass permitted by the spacecraft require an areal density of the mirror segments of roughly 1 kg/m^2. For the mirror substrate, we have been using a glass from Schott, D263 (with density ~ 2.5 x 10^3 kg/m^3). The thickness of these mirrors is therefore limited to approximately 0.4 mm. Within these broad parameters, the critical challenge in the optics thus lies in attaining the angular resolution with these thin glass mirrors, and to produce, align and mount them within schedule.

Optics for EUV, X-Ray, and Gamma-Ray Astronomy IV, edited by Stephen L. O'Dell, Giovanni Pareschi, Proc. of SPIE Vol. 7437, 74371D · © 2009 SPIE
CCC code: 0277-786X/09/$18 · doi: 10.1117/12.825105

The mission requirement on imaging of the telescope is 5 arc-seconds, measured in half-power-diameter (HPD). This requirement necessarily flows down to an even tighter requirement at the individual mirror level. Currently, the error budget allocates 2.4 arc-seconds for individually mounted mirror. The central technologies that are needed to be developed to meet these requirements, specifically, are therefore: first, to develop a glass forming/slumping technique that allows fabricating mirror at the allocated 2.3 arc-seconds level with glass of thickness of 0.4 mm; and secondly, to develop a mirror handling technique which allows aligning and mounting these lightweight mirror segments with sub-arc-second mounting error. These mirror segments can be thermally formed on precise mandrel. The forming process aims for the glass segment to take up precise low order figure. High-frequency surface properties, which is inherent in the glass and is acceptable from the original smooth glass substrate, is preserved in the thermoforming. (For the development of glass slumping for IXO mirrors, see reference [5].) The mounting processes include mounting the mirror for metrology, as well as enabling them to be aligned and integrated. In this paper, we will focus on the effort, at NASA's Goddard Space Flight Center, to meet these opto-mechanical challenges posed by the thinness of the mirror segments.

1.1 Baseline design of IXO soft x-ray optics

To meet the mission requirements, a baseline telescope design was developed in which the telescope is 3.3 m in diameter (diameter of outermost mirror shell inside the 3.3 m envelope is 3.2 m), with a focal length of 20 m. The design of the telescope's construction is modular. It consists of 60 modules, in 3 radial sections. There are 12 inner, 24 middle and 24 outer modules. Each module consists of from 100 to 140 mirror shells (and twice that many mirror segments). The radial breaks of the sections are chosen for optimal optical throughput and also from the consideration that the mirror segments, nominally 15° or 30° in angular span, are not wider than 400 mm. The widths of the mirror segments range from 200 to 400 mm. The length of the mirror segment is 200 mm for each stage of primary and secondary x-ray reflection. Given this axial length of 200 mm, 1 μm error peak-to-valley in low order axial figure error, for example, in sag, results in an error of 2 arc-seconds in the mirror's axial slope, or 4 arc-seconds in reflected rays. This is further compounded, in double-reflection, with a similar error from the secondary mirror. The limit on the amplitude of figure distortion is even more stringent for error of higher spatial frequency. The thin mirrors are therefore to be aligned and mounted, in the telescope housing, with precision in displacement at a level below a micrometer.

2. MIRROR FIGURE DISTORTIONS

Two of the major sources of mirror figure distortion in mirror mounting are gravity sag and thermal distortion (for our purpose, other source of errors, such as distortion from coating stress of film deposited for x-ray reflection, is considered inherent in its "forming" and is part of the mirror. We also assume the form of the mirror is not changing in the time scale of interest.) Even though there is no gravity distortion when the telescope is in space, important issues arise from mounting mirrors for metrology, assembly into the telescope housing, ground test, and gravity relief after launch. The mirrors, depending on how they are affixed into the telescope housing and the mirror assembly's thermal control, will suffer from strain arising from CTE (coefficient of thermal expansion) mismatch, and temperature non-uniformity due to uneven heating as well as thermal lag in getting to thermal equilibrium.

2.1 Thermal stress

The material for the mirror housing currently under consideration is an titanium alloy Ti-15Mo, whose CTE is measured to be 7.8×10^{-6} /°C at room temperature range. The CTE of the glass we currently are using, Schott D263, is 6.2×10^{-6} /°C. Depending on how the mirrors are bonded to the housing, the degree of thermal distortion may differ. Nevertheless, as long as the mirror is fixed to a rigid structure, or to a structure that is much stronger than the mirror, as is typically the case, the mirror's thermal distortion is largely dependent on their relative thermal strains. Thermal strain of the glass mirror and its housing structure is $\varepsilon = \alpha\ (T - T_0)$, where α is the coefficient of thermal expansion, and T is the part's temperature, T_0 is a common reference temperature when no strain between the mirror and the structure occurs (for example, a common temperature when the mirror is being affixed to the structure). The differential strain of the mirror with respect to the housing structure is therefore $\Delta\varepsilon = \Delta\alpha\ (T - T_0) + \alpha\ \Delta T$, where $\Delta\alpha$ is the CTE mismatch between mirror and the structure, and ΔT is the temperature difference between them. That is, the source of thermal stressing is two-folded: that from a bulk temperature change with different CTEs between the glass and the housing materials, and a temperature difference between the mirror and the external structure it attaches to.

Analytical structural-thermal-optical-performance (STOP) studies were done to evaluate the thermal effects. The model consists of 135 pairs of mirrors, with radius from 372 mm to 671 mm, in a telescope module. These mirrors correspond to those in the inner module in the IXO telescope's baseline design. The module structure comprises housings of two stages, each of which has a front, a back, two side panels, and eight rails. The mirrors are fixed to the rails, three on each side and at middle at the top and bottom. Mechanical-thermal finite element analysis was run for various cases of thermal conditions. The mirror displacements were subsequently fed into an optical calculation to produce the degradation of HPD expected from the deformation of such surfaces. It is found that, for bulk temperature rise with a CTE mismatch, HPD degrades at 3.0 arc-second /°C for a $\Delta\alpha$ of 1 ppm/°C (10^{-6}/°C); and for materials with matched CTEs, HPD degrades at 20 arc-second /°C for bulk temperature difference. Both of these are consistent with an HPD dependence of Δ(HPD)/$\Delta\varepsilon$ of about 3.2 arc-second/ppm. The thermal dependence of surface distortion was measured in an experiment in which a mirror was bonded on a CTE-matched strongback (similar but different boundary conditions: a single mirror of radius 240 mm, bonded at only 4 points). The experimental result was that additional axial sag arises from thermal stressing, at the level of 3.3 μm/°C, which will contribute to an HPD degradation of approximately 13 arc-second/°C, or an Δ(HPD)/$\Delta\varepsilon$ of 4.2 arc-second/ppm of strain. Furthermore, the figure error of sag from the primary and secondary mirrors will combine to contribute to an even larger error. A series of experiment and analysis for glass mirrors on Ti strongback is ongoing, to better understand the thermal stress under different conditions and also for model verification. Preliminary result is consistent with 10 arc-second/°C in temperature difference. So the experimental result is quite consistent with the model prediction, and points to a high temperature sensitivity of 3-4 arc-second for each ppm of thermal strain, for the boundary conditions under consideration.

Figure 1. Model for the structural-thermal-optical-performance analysis consists of 135 pairs of mirrors in an IXO module, consisting of a primary and a secondary stage. Mirrors are modeled as shells in a mesh of 21x21 nodes per shell. Finite element displacement and angle variables are fed into optical calculations, to evaluate the optical performance, in particular, the HPD.

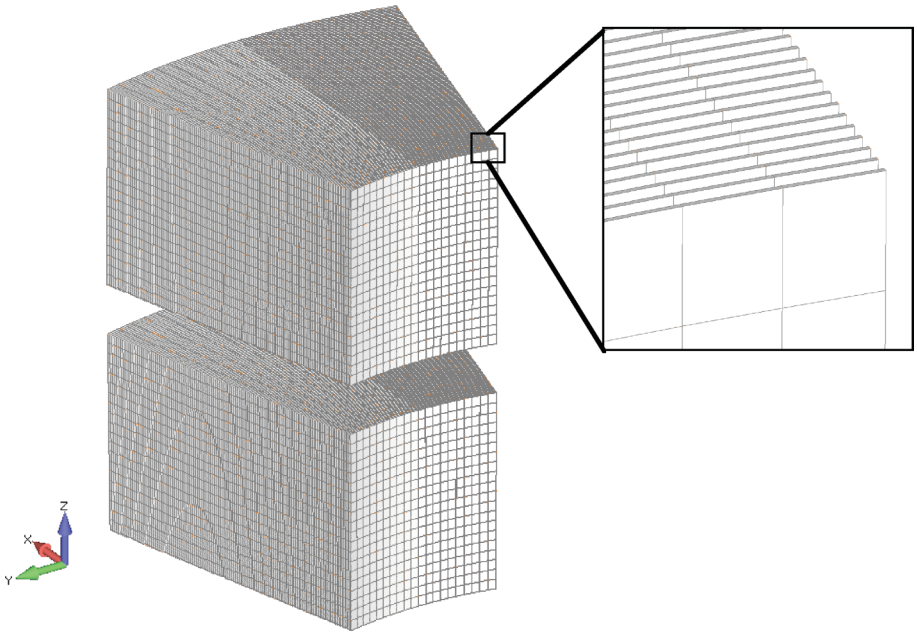

Given that the image degradation from thermal strain is (3-4) arc-second/ppm, a limit can be placed on the bulk temperature change allowed of the telescope. To limit the image degradation from thermal stress to 1", and for a CTE mismatch between Ti and the Schott D263 glass of 1.6 ppm/°C, the tolerance on the telescope's operational temperature is no more than about 0.2°C from the base temperature, at which the mirrors are originally mounted. Mounted this way, the requirement of temperature gradient between the mirror and its local structure is about 0.05°C. Alternative affixing method that does not strain the mirror as much axially, or structural designs that includes athermalization concepts, may be needed to relax these thermal constraints. For instance, properly designed built-in flexure at the attachment point where the mirror meet the housing may help to absorb part of the thermal stress.

2.2 Gravity sag

Gravity sag of mirror in ground operation, as well as gravity relief in space, poses a significant problem for mirror mounting and testing. For example, the magnitude of gravity sag for a flat plate with rectangular cross-section, supported at or near the ends, typically is $\Delta = (f/32)\sin(\alpha)\,(\rho g/E)\,(L^4/\tau^2)$, where Δ is the maximum sag near the middle of the plate (ρ is the density of the material, g the acceleration due to gravity, E the Young's modulus of the material, L the length and τ the thickness.) Angle α is that of the plate to vertical. The factor f is generally of the order of unity, and it depends on the types of supports and the locations of the supports. For typical values of the IXO mirrors, the gravity sag is generally too large except for small angle α (for instance, 1° or less.) We should note that the approximation is not good for axial sag near the middle of the mirror, as it cannot be bent like a plate is. Nevertheless, to reduce the gravity distortion without violating other constraints such as the dimension and thickness, we are left with the following options: optimizing the strategic locations and significantly increase the numbers of the mounting points (or even extending them to be 1-dimensional edges); or keeping α small by the orientating the mirror vertical. We will primarily consider a process in which the mirror is oriented vertically.

3. SUSPENSION MOUNT

3.1 General Considerations

To mount the mirror, a number of approaches can be taken. One can take an active alignment approach in which the mirror figure is "fixed" by adjusting it at or near its mount points, before affixing it onto the structure. One can also take a more passive approach in which the mirror is forced into a prescribed precise geometry. One can take an even more passive approach in which all the mounting and alignment processes aims not to improve or disturb the formed mirror in any way. All three approaches are in principle workable and indeed are being pursued for mounting the IXO mirrors. For the first approach, an implementation, taken up by a team at the Smithsonian Astrophysical Observatory, employs actuators[6] at ten points at the fore and aft ends of a mirror in order to tune the mirror's low order figure, especially its axial tilt angles. This potentially can be used to optimize the mirror's focus. An implementation of the second approach, taken up primarily at ESA and associated industries, is to press mirrors, which are made of silicon wafers with precisely etched ribs, onto each other, and eventually build up a mirror module[7]. The shape of the mirror (silicon wafer) is deformed, especially in the azimuthal direction, in the process with prescribed parameters. Taking the third approach, we at NASA's Goddard Space Flight Center and collaborators attempt to take thermally formed glass mirrors, and to mount them without introducing significant distortion[8]. Our goal is to align and mount the mirror so that the optical figure of the mirror segment is preserved. The process must also provide sufficient mechanical stability such that the mirror segment can withstand the launch load without any degradation of performance[9]. One advantage of this approach in terms of technology development is that it naturally separates the tasks of mirror figuring from mirror mounting, and the two processes can be developed more or less independently.

To be more specific, our approach, which we call a "suspension mounting approach" is currently implemented in the following fashion. (1) A given thermally formed mirror is suspended at two or more points by strings, so that the middle meridian, or the bulk of the mirror is vertical. This orientation minimizes the force of gravity normal to the mirror surface. (2) The suspended mirror is temporarily affixed to a strongback---a stiff structure made of the same material, or material with the compatible CTE---in a fashion such that all the forces involved in this fastening is sufficiently small so as not to distort the mirror. At this point of the development, we use pins floated in near-frictionless air-bearings to achieve the small (sub-milli-newton) force. The bonded pair---the mirror and its strongback---now form a rigid body, and can then transferred and situated for metrology, alignment and further processing. (3) The mirror on its strongback can now be transferred to the module housing, be aligned optically to achieve proper focus, and be bonded onto the module housing. The temporary bonds can subsequently be removed and the mirror dismounted from the strongback. In the following sections, we will discuss the procedure and accuracy of each of these steps.

3.2 Suspension

The simplest suspension method is a 2-string suspension, in which the mirror is simply suspended at two points at one end of the near-conical mirror segment. For a symmetric configuration, the separation of the suspension point is uniquely determined to ensure that the center of gravity is in the same vertical plane containing the suspension points. For example, for an ideal thin circular arc with radius R and angular span Θ, the chord length separating the suspension points is $L = 2R\sin(\Theta/2)/(\Theta/2)$, or $2R\,\mathrm{sinc}(\Theta/2)$. For a realistic mirror, the suspension is similar except for a small

correction due to a non-zero mirror thickness and the conical (non-cylindrical) nature of the mirror. In practice, we glue kelvar strings to the top end of the mirror with this separation. For the dimension of mirrors under studied, sufficiently precise L can be obtained in practice to assure that mirror tilt is better than, for example, 0.1°. Precision of L necessarily depends on the size and cone angle of the mirror segment. Finite element modeling shows that mirror distortion is negligible for such small angular tilt.

Nevertheless, self-gravity sag of the mirror in its tangential direction (approximately vertical in this orientation) is not negligible. Even though the distortion in this direction is very small, it is not energetically favorable for the distortion to be sheared entirely "in-plane". The mirror responds to this gravity sag by "curing up" to create an azimuthally varying tilt, corresponding to a focus error in the focal plane. Similar gravity sag along the mirror surface occurs regardless of whether the mirror is one in the primary or secondary stage with different cone angles, the detailed of intrinsic axial curvature, or for that matter, whether it is a cone or a cylinder. For example, for a mirror with a radius of R = 242 mm, Θ = 50°, the variation of angular tilt can be as much as 2 μm rms over the 200 mm mirror length. This corresponds to a focusing error of about 8" rms. However, unlike the sag error, the same suspension error occurring on the primary mirror and the secondary mirror will cancel each other. Second (axial sag) or higher order error from the two-string suspension is negligible.

Figure 2. Suspension of a mirror with two strings is shown in the left panel. The suspending strings are attached to the mirror at prescribed points so that the mirror center meridian is vertical. The mirror is then bonded, at its back, to a strongback (in this case, at 4 points.) The right panel shows a model of the mirror in suspension. There is a variation of mirror axial tilt as a function of azimuth. Second order distortion, or axial sag, is negligible.

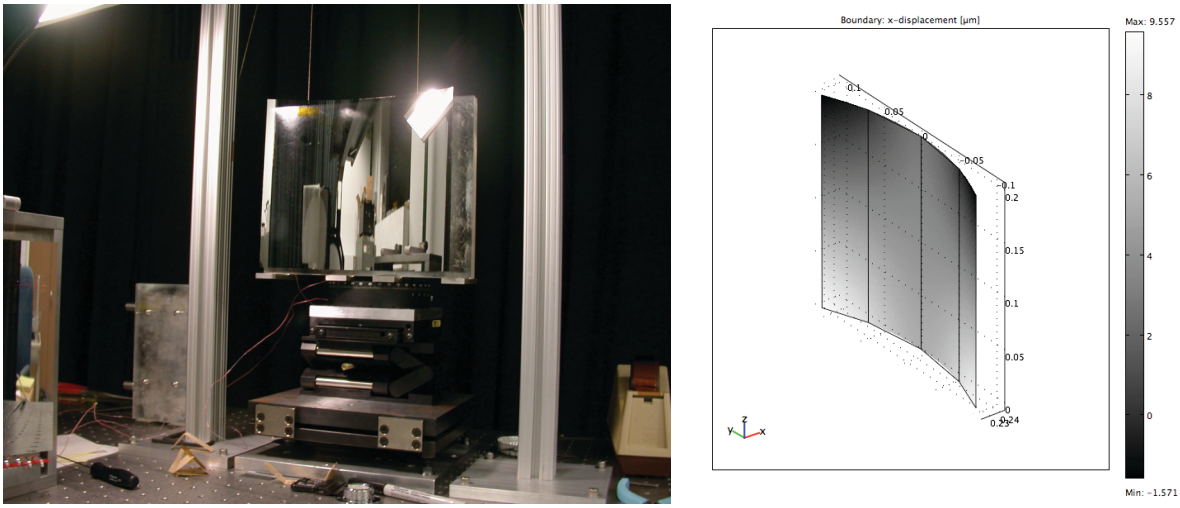

To further minimize figure distortion from suspension the mirror, more suspension points can be used. For example, a 4-string configuration can be used. A whiffle-tree implementation of a 4-string suspension, with crossbars for each pair of strings, will effectively reduce the distortion by re-distributing the load to more azimuthal positions at finer spatial scale. (A simple direct 4-string suspension is statically indeterminate, and fine adjustment of string lengths, especially stiff ones, or tension of strings, is needed.) In the whiffle-tree implementation, the tension of the strings are self adjusting (to one-quarter of the weight of the mirror). Like its 2-string version, the positions of string attachment are necessarily constrained in order to have the center of gravity properly placed for the mirror be vertical. We have started an investigation to demonstrate this improvement. Result will be reported elsewhere.

3.3 Temporary Transfer Mount

To test the mounting methods, we fabricated CTE-compatible glass strongback for mounting mirrors. These are made by fusing sheets of the same glass as the mirror, in order to separate the complication with CTE mismatch. We also have fabricated Ti strongbacks for the same purpose. As pointed out before, mirror bonded to a Ti strongback, which has a similar, but not exact CTE as the glass, can have an error due to thermal stressing. Nevertheless, machining of the metal strongback can be much easier, be done more precisely and the structure can be made into much more sophisticated form. The glass strongbacks are flats or curved structures having a number of pins for a mirror to be bonded to their tips.

The number of pins ranges from 4 to 16, but we primarily experimented with a 4-pin or 8-pin set up currently. In order to capture the figure of the suspended mirror without introducing additional distortion, the pin can only impart a small force to the mirror. From finite element analysis, for 4-pin mounting at general position not too close to mirror's corner, force normal to the mirror surface is limited to < 1 mN in order not to distort the mirror in its sag. The force to alter a mirror's local tilt angle is even smaller for a 4-pin mount. Two experimental approaches were investigated: (1) Direct bonding with epoxy of mirror onto tips of adjustment screws with fine pitch (25 μm thread was used), where the screw lengths are pre-set to match the mirror at its back; (2) Bonding onto pins in low friction bearings.

Direct bonding of mirror onto strongback is straightforward and have achieved good repeatability for 4-pin mounts. Some of the early results were reported previously[8]. In this simple scheme, a mirror in suspension is brought to contact with the pins on the strongback to within ~ 0.2 mm. The mirror and the strongback are then separated before epoxy beads, which have a typical size of 1 mm, are applied at the tips of the pins and the mirror is brought back into contact with the pin again. However, extending this procedure to more pins in order to facilitate the transfer to an external structure encounters some difficulty. The direct insertion of a bead of epoxy to bond the mirror to the pins causes displacement of the mirror relative to the pins, and it shows up as a variation in axial tilt angle in a simple rectangular style 4-pin bond and higher order figure error in a configuration with more than 4 pins. The induced displacement is caused by a combination of the non-uniform size of the epoxy beads, uneven epoxy shrinkage and surface tension of the adhesive.

Figure 3. A pair of mirrors bonded to fixed pins are shown in the left panel. The mirrors were bonded with direct insertion of epoxy between the mirror and the pins. The strongbacks are made of titanium. On the right panel, a mirror is bonded to pins floated in air-bearings. Pins floated in housings, with compressed air at 30 psi, can be displaced by mm with a force of just a few 10^{-4} N.

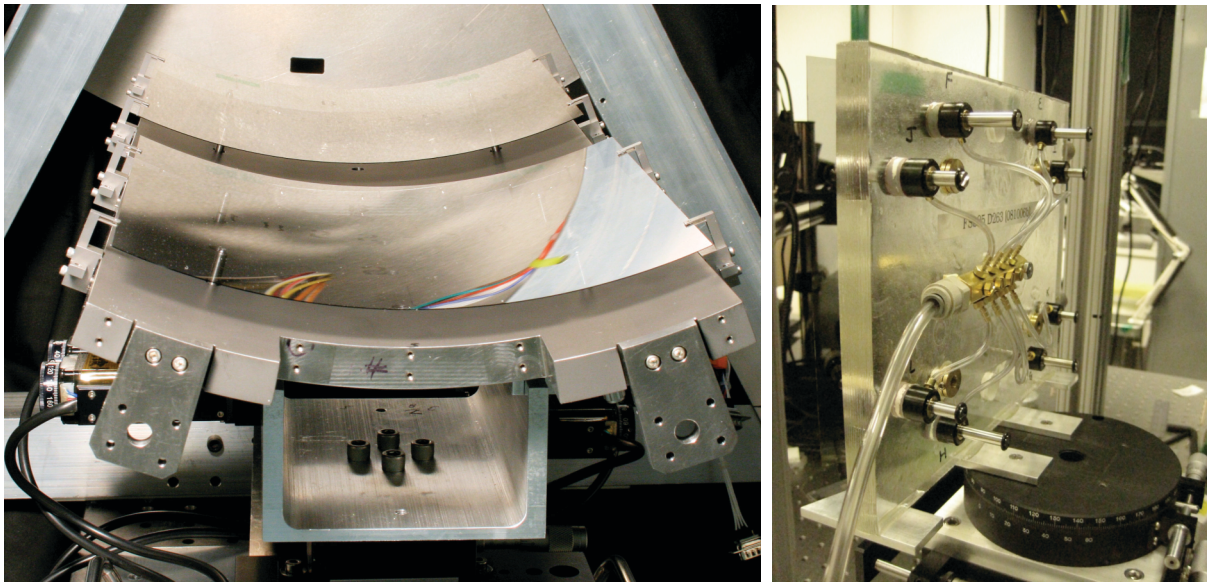

To reduce the impact of epoxy, a better method is to get around this "epoxy-filling" effect by first bonding the mirror onto pins that are "free", so that the any change in the bond line can be accommodated. The pin is subsequently fastened onto the external structure in any mechanism operating radially on shaft of the pin, thereby without needing to affect the pin in the direction normal to the mirror surface. For the choice of pins of suitable sizes, given a typical coefficient of friction of 0.5, say, between aluminum and steel, a pin having a mass of 0.2 g and with a diameter of about 1 mm is required in order for it not to exert a force normal to the mirror surface just from frictional force. It turns out that a pin this small is not strong enough to hold the mirror in place. The bending of the pins after the removal of the suspending strings imparts bending moments local to the bond points. These local moments from pin-bending were demonstrated in surface metrology of mirrors bonded this way. Stronger pins sliding on ball bearing, thus having smaller coefficient of friction, is another option. We tested a set of linear bearing with pins of 2.7 g in mass and 3 mm in diameter. The coefficient of friction was smaller and measured at 0.12, but because of the larger mass, the frictional force is still appreciable, at about 4 mN normal to the mirror surface.

A set of air bearings provides very little friction to bonding pins. These work with larger pins with 6.35 mm in diameter. The pins are floated in their housings with sheaths of air cushion in tight gaps of approximately 10 μm. The "friction", measured from the angle that the pins begin to slip in either direction from its neutral position, is small ~ 0.002, if it is at all measurable. However, imbalanced air-flow, from imperfection in machining the tight gap where air flows, causes the pins to move forward or backward simply by air-dragging. By lightly polishing the pins, we were able to established equilibrium states of the pins so that they can be stable, and will gently oscillate about their equilibrium positions. Precise setting of the equilibrium positions and gentle profiling of the pins can ensure very small force from the pins onto the mirror. The restoring force is estimated, from the periods of oscillation, to be 0.1 – 0.4 mN/mm. More direct measurement with force gauge coupled to pins on air bearings demonstrated forces as small as 0.016 mN/mm over nearly the entire length of the pin and is essentially linear. Some pins are not as good due to difference in machining. Nevertheless, such force is sufficiently small for our application.

With the set up, a mirror was bonded to the pins floated in these low friction bearings. The procedure was repeated five times, from which very good repeatability and small distortion of low order figure was achieved (besides in one case that there was an operational incidence, the other four cases were shown in figure 4.) The second order error is shown to repeat particularly well. The fastening mechanism of the pin to the strongback is still to be improved upon. Various mechanisms from bonding to cramping are being continuously investigated.

Figure 4. Low order parameters characterizing a mirror bonded to pins with air-bearings. The mirror radius is nominally 242.5 mm and spans 50 degrees. Bondings are done at four points, with two in each azimuths where the mirror was first suspended. Dependence on azimuthal angle of radius variation, tilt angle variation and axial sag, are shown.

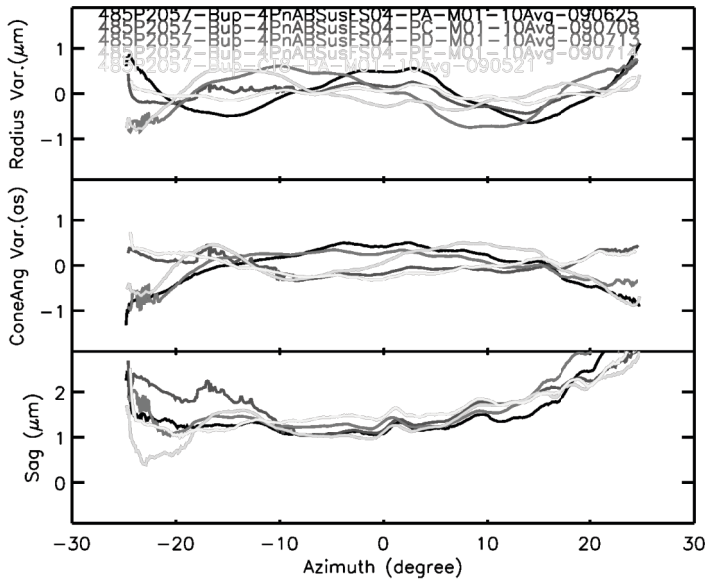

3.4 Permanent Mount onto Mirror Housing Simulator

The process of aligning mirrors on the temporary mount, and subsequent transferring of them from the temporary mount to a permanent structure is studied with the aid of a Mirror Housing Simulator. This simulator is a framed structure made of titanium, Ti-15Mo, and consists of bonding tabs, also made of titanium, on short rails at its sides (and top and bottom ends.) The simulator consists of two stages.

A mirror housing simulator structure was designed, modeled and fabricated. It can accommodate 3 pairs of mirrors of different radii. It is kinematically mounted in the vertical orientation on its base plate. Mirror to be bonded onto the housing simulator is transferred from a strongback where the mirror is temporary-bonded. Mirror bonded on the strongback in the temporary mount can be oriented and aligned with the aid of a 6 degree-of-freedom hexapod. The mirror will then be de-bonded from the strongback. The de-bonding process was tested repeatedly in test fixtures and was shown to be reliable. For the mirror bonded onto the pins in the strongback, a small twist of the pins will cause the mirror to be detached from the pins without any measurable damage. Alignment and bonding of mirrors onto the housing

simulator are in progress. X-ray testing of these mirrors are planned. To test the permanent bonding and the mirror transfer processes, simulation of the process was carried out with a series of mirror strongbacks, in which a mirror temporary-bonded in the strongback is transferred onto itself. The transfer processes include bonding the mirror at its periphery to tabs on the strongback, as if it is a telescope housing, and de-bonding the mirror at its temporary bonds. The mirror was then qualified with both surface metrology and x-ray testing.

Figure 5. The mirror housing simulator. The framed 2-tier structure, made of Ti-15Mo, is shown on the left panel. The right panels shows a detailed view of the tab mechanism for bonding aligned mirror.

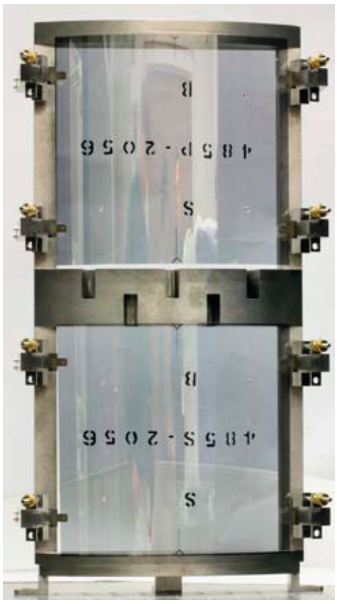

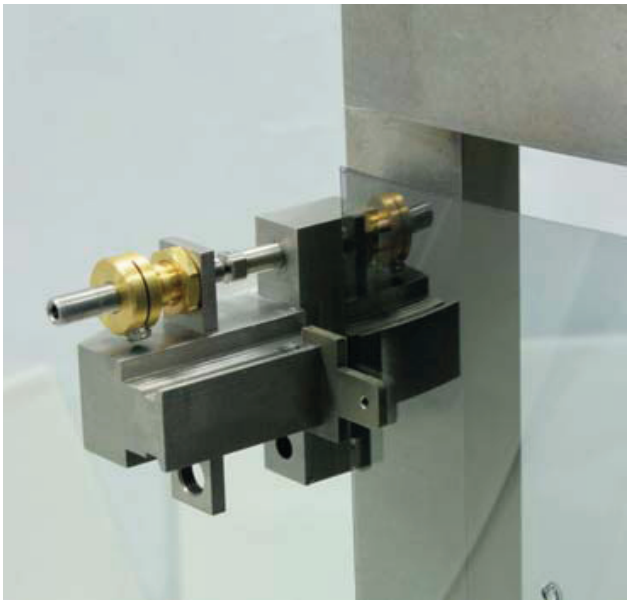

4. RESULT AND DISCUSSION

4.1 X-ray test

To test the concept of the mounting scheme described above, we carried out the suspend-transfer-bond processes for 4 sets of mirrors, and assessed the imaging performance of them in x-ray. In these tests, carried out from November 2008 through March 2009, we suspension-mount a primary and a secondary mirror onto glass strongbacks, transferred the mirrors onto itself as described above, and bonded the mirrors at the stronngbacks' edges. These procedures mimic the processes that can be used for mounting mirrors onto telescope housings. The mirrors are subsequently aligned to achieve focusing at the nominal focal distance. For historical reasons, all of our mirrors are of 8.4 m focal length, as the mirrors are fabricated with heritage mandrels with a f = 8.4 m design. We note that, in our procedure, the alignment follows the bonding of the mirrors; whereas in the actual implementation conceived, the bonding occurs after alignment. The error associated with this difference in procedure is not included in our tests. They will be included in the upcoming tests for mounting mirrors in the mirror housing simulator. Four series of mounting, alignment and measurements were carried out. Except for one test in which the strongback was inadvertently distorted from an inappropriate mechanism for mounting the strongback itself, the other three are listed in Table 1.

X-ray tests were carried out at the 600 m beam line at Goddard Space Flight Center. Due to the finite distance of the x-ray source, a beam divergence correction of $\sim f/L_B$ of 1.4% was made to the focal distance. X-ray tests were first carried out at three different energies: Al Kα at 1.5 keV, Ti Kα at 4.5 keV and Cu Kα at 8.0 keV. From the first measurements, it was verified that for the angle of incidence under consideration (0.42°), the dependence of mirror imaging performance on x-ray energies was not significant at the current level of imaging quality. Subsequent tests were therefore only carried out at a single energy, which was chosen, for practical purpose, to be the Ti line at 4.5 keV. Detection is done with a Princeton Instrument 1024 x 1024 pixels x-ray charge-coupled device, operating at about -

100°C. Several attempts of alignment were made for each pair of mirrors, and their corresponding x-ray images were taken. The range of values listed in the table reflects the statistics of these measurements.

Table 1. A summary of x-ray tests of suspension mounted mirrors.

Test Date	Mirror, Strongback & mounting conditions	Half-Power Diameter (arc-sec)	90%-Power Diameter (arc-sec)	Best HPD (arc-sec)
11/12/2008 – 11/20/2008	P2009/S2009. 4-point temporary bond at suspension azimuths. Mirrors face sideways.	1.5 keV: 19.77 ± 0.21 4.5 keV: 19.19 ± 1.11 8.0 keV: 17.81 ± 1.39	1.5 keV: 62.0 ± 4.5 4.5 keV: 57.9 ± 3.3 8.0 keV: 53.3 ± 5.7	16.6”, 16.8”
02/12/2009 – 02/19/2009	P2021/S2024. 4-point temporary bond at suspension azimuths, transfer to 4-point permanent bonds at edges. Mirrors face up.	4.5 keV: 19.62 ± 1.24	4.5 keV: 52.7 ± 3.8	16.6”, 17.2”
02/28/2009 – 03/01/2009	P2021/S2041. 4-point temporary bond at suspension azimuths, transfer to 4-point permanent bonds at edges. Mirrors face up.	4.5 keV: 18.67 ± 1.25	4.5 keV: 47.1 ± 2.5	16.6”, 17.9”

Figure 6. Summary of an image and the performance of a bonded pair of mirrors, tested on 3/1/2009. The panels show the image in the detector plane (top left, detector pixel is 13 μm square); determination of the image center in the long direction from width of image slices (top right); photon radial density distribution as a function of radius (bottom left); encircled energy function and the half-power diameter (bottom right).

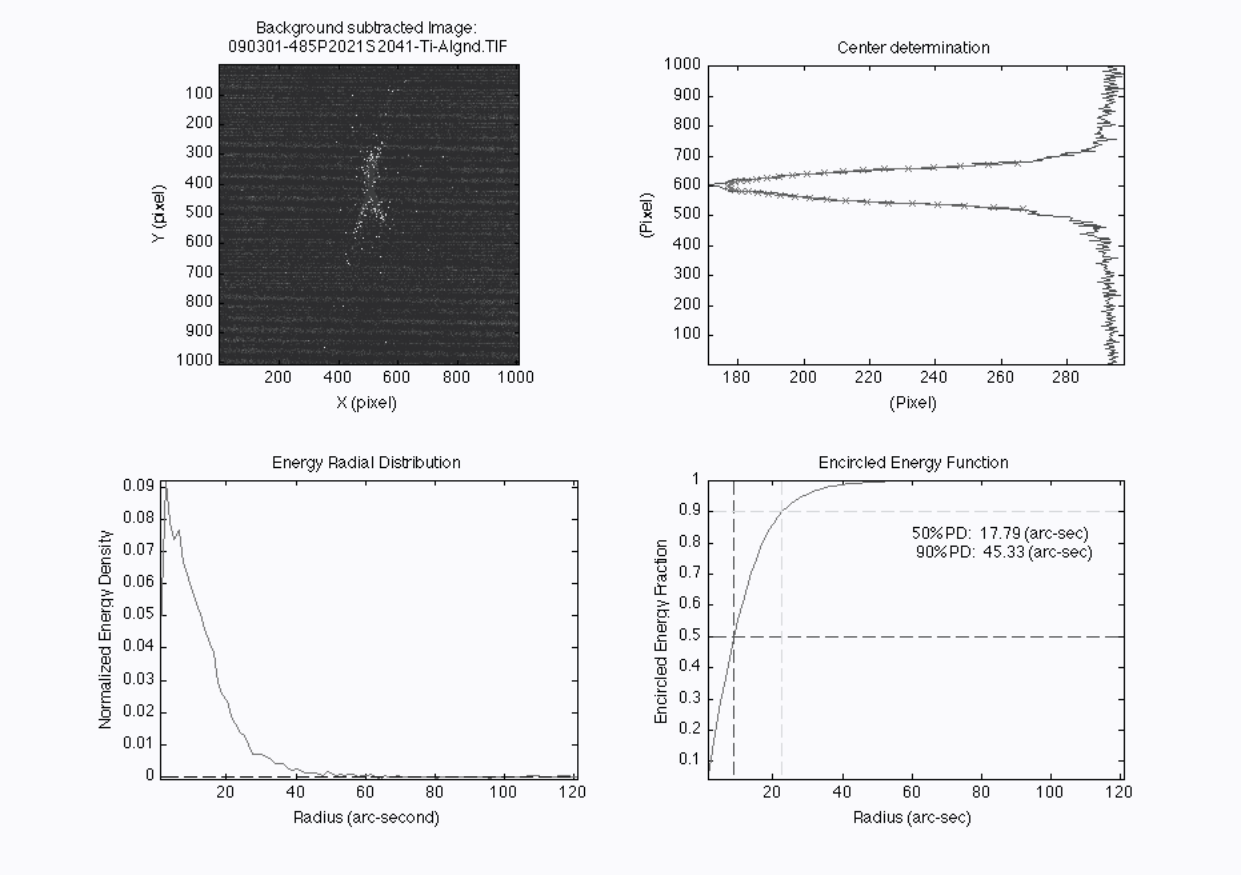

The mirror's performance, of which the angular resolution is our prime concern, was derived from a determination of the center of the image and with that the encircled energy function. An example is shown in figure 6. The center of the image is determined as the "neck" of the image, or alternatively, as the position having the peak intensity. Either of these methods yields similar results and the uncertainty associated with this determination is < 1 arc-second. The difference in HPD due to this uncertainty is much less than one arc-second. The derivation of the x-ray imaging performance, however, is susceptible to detector background as well as its treatment in analysis. Depending on the detector background noise, x-ray intensity, collecting time, and treatment of background analysis, values of the HPD derived can be different to about 10%. Since the signal is only a small fraction of the total background, and the image size is relatively small compared to the area of detector to be considered for background analysis (we chose 2 arc-minutes for the analysis of background, the detector size is over 5 arc-minutes), the cumulative background counts can easily overwhelm the signal in the consideration of the encircled energy function. For the values listed in the table above, we chose a method that attempted to fit the background with a 2-dimensional quadratic form. A smaller HPD values, up to 1.5" smaller, can result if we chose different approach to analysis, such as a smaller area to analysis, and assume different constants for the background (some "background" pixel may become negative). The "best HPD" listed in the table reflects those choices. The average values in Table 1 include all the data in full image measurements, and should be considered as a rather conservative estimate of the overall performance of the process. Better results were demonstrated in selected measurements.

Detailed analysis of the P2009/S2009 mirror pairs was carried out, with optical surface metrology of the mirror before and after temporary bonding and permanent bonding, and after the x-ray test. Differencing in those map showed that the additional errors due to figure distortion introduced in the mounting process is about 8 arc-seconds. This error is currently better than that of the intrinsic mirror figures themselves but is not sufficient to meet the mission requirement, especially now that the mission requirement of the telescope's angular resolution is re-defined from Constellation-X's 1 arc-second to IXO's 5 arc-second. The present mounting performance would have been very close in meeting the original pre-IXO (i.e., Constellation-X) mission requirement.

4.2 Plans for Technology Development

As stated, our goal for the "suspension mount" is to use the precision figure of the mirror segment as the starting point, and seek to preserve the mirror's figure in the mounting process. The procedure can generally be divided into three components: First, the suspension and mounting of mirror which aims to ready the mirror and capture its "free-state" onto a strongback; second, metrology and alignment of the mirror possible now with the mirror on its strongback; third, transfer and bonding of the mirror onto the telescope housing and dismounting/de-bonding of the mirror from its temporary structure. As of now, development of the three technology components is pursued nearly independently and in parallel, as is reported above. We have begun testing with bonding at just 4 pins, and the plan is to move to bonding at larger number of points for more secured mounting. Numerical and experimental studies indicated that a bonding at 8 points around the mirror perimeter would be sufficient[9]. In fact, bonding at more than eight points may not significantly enhance the margin against structural failure, but it may distort the mirror figure unnecessarily, and at smaller spatial scale.

We are conducting intense studies on critical issues related to each of the three components above. They include: gravity sag from suspending the mirror; displacement of mirror due to the bonding processes, such as during epoxy application, from the adhesive's viscosity and surface tension effects, and epoxy shrinkage; and thermal stress and strain. We hope to achieve the following technology readiness in four overlapping phases. In phase A, we temporary-bond mirror segments at 4 points to a strongback, with optical metrology and x-ray test as verification. In phase B, we temporary-bond and transfer mirror segments at 4 points to a permanent structure, again, with surface metrology and x-ray test to evaluate the performance. In phase C, we extend the process to bonding at 8 points. Finally, in phase D, we will co-align multiple pairs of mirror onto the housing structure, and conduct x-ray tests as well as vibration and acoustic tests for process qualification. As of now, we have gone through large part of phases A and B, even though more improvement in terms of precision is planned. Studies in phases C and D have started.

4.3 Summary

In summary, we have developed the suspension mount, a passive approach to mounting the mirror without attempting to actively adjust for the mirror's figure. We have developed different aspects of the suspension mount: the suspension, the temporary-bond, transfer and permanent bond, in parallel, and to an extent that the combination of the developed techniques produce mirror pairs of an HPD of 16 arc-second, tested in full beam x-ray tests. The error component in

mounting the pair was estimated from surface metrology as 8 arc-second, whereas the mirror itself is about 11" each. We have planned further improvement of the techniques, including using a near frictionless air-bearing in the temporary-bond; 4-string whiffle-tree suspension method to reduce distortion due to the suspension; mechanical design with flexures, of kinematic mounting of the temporary strongback to take out its other mechanical distortion. We have designed and fabricated a housing simulator for the purpose of experimentation of mirror transfer and alignment.

REFERENCES

[1] Bookbinder, J., "The International X-Ray Observatory: Activity submission in response to the Astro2010 Program Prioritization Panel RFI," Internal and submitted document in response to the Astro2010 Decadal Survey (2009).

[2] Bookbinder, J., Smith, R., Hornscheimier, A., et al., "The Constellation-X Observatory," Proc. SPIE 7011, 701102 (2008).

[3] Kibourne, C., Boriese, W., Bandler, S., et al., "Multiplexed readout of uniform arrays of TES x-ray micro calorimeters suitable for Constellation-X," Proc. SPIE 7011, 701104 (2008).

[4] Zhang, W., Bolognese, J., Byron., et al., "Constellation-X mirror technology development," Proc. SPIE 7011, 701103 (2008).

[5] Zhang, W., et al. "IXO Mirror Technology Development," Proc. SPIE. Volume 7437 (2009).

[6] Podgorski, W., Caldwell, D., Freeman, M., et al., "A mounting and alignment approach for Constellation-X mirror segments," Proc. SPIE, 7011, 701112 (2008).

[7] Bavdaz, M, Lumb, D, Wallace, K, et al., "Large effective area high angular resolution x-ray optics," Proc. SPIE 7011, 701109 (2008).

[8] Chan, K-W., Zhang, W., Saha, T., et al., "Opto-mechanics of the Constellation-X SXT mirrors: Challenges in mounting and assembling the mirror segments,", Proc. SPIE 7011, 701114 (2008).

[9] Freeman, M., Reid, P., and Davis, W., "Design study for support of thin glass optical elements for x-ray telescopes,", Proc. SPIE 7011, 701113 (2008).